significant differences between $P_M(\phi,x)$ and $P_T(\phi,x)$ lead to R_M and R_T results which are not significantly different for any practical purpose.

The present results indicate that although G_{PT} and G_T depend on ϕ differently and G_{PT} should be superior to G_T, their differences actually lead to P_{NN} and R_{NN} results which are far too close together to allow any discrimination. As far as R_{NN} is concerned, it makes no significant difference which of the four $G(\phi,x)$ choices is used. Although the best choice for P_{NN} for the CS EOS seems to be P_{TC}, the use instead of P_r induces only negligible differences and has the virtue that the required $g_r(\phi,1)$ function is immediately available from this or any other EOS of interest.

Conformational Equilibrium in the Alanine Dipeptide in the Gas Phase and Aqueous Solution: A Comparison of Theoretical Results

Douglas J. Tobias† and Charles L. Brooks III*

Department of Chemistry, Carnegie Mellon University, Pittsburgh, Pennsylvania 15213
(Received: November 4, 1991)

The acetyl and methyl amide blocked alanine amino acid, commonly referred to as the alanine dipeptide, has often been used as a model in theoretical studies of backbone conformational equilibria in proteins. In order to evaluate the solvent effects on the conformational equilibrium of the dipeptide, we have used molecular dynamics simulations with holonomic backbone dihedral angle constraints and thermodynamic perturbation theory to calculate free energy profiles along paths connecting four important conformations of the dipeptide in the gas phase and in water. We found that the extended β conformation is the most stable both in the gas phase and in water. The C_{7ax} conformation (seven-membered ring closed by a hydrogen bond with axial methyl group) is less stable than the β conformation by 2.4 kcal/mol in the gas phase and 3.6 kcal/mol in water. The right- and left-handed α helical conformations, α_R and α_L, are less stable than the β conformation by 9.1 and 11.6 kcal/mol, respectively, in the gas phase. However, in aqueous solution the α_R and α_L conformations are less stable than the β conformation by only 0.2 and 4.1 kcal/mol, respectively. Thus, we found, as others have previously, that there is a marked solvent effect on the backbone conformational equilibrium. We have determined the energetic and entropic contributions to the free energies to explain the relative stabilities of the dipeptide conformations in terms of differences in peptide–peptide and peptide–solvent interactions. Finally, we have compared our results to the results of several previous theoretical studies of the alanine dipeptide.

Introduction

The alanine dipeptide[1] (see Figure 1) has served as a paradigm for theoretical studies of backbone conformational equilibria in proteins. This is because the dipeptide contains many of the structural features of the protein backbone (the flexible ϕ and ψ dihedral angles, two amide peptide bonds whose NH and CO groups are capable of participating in hydrogen bonds with each other and with polar solvent molecules, and a methyl group attached to the α carbon that is considered representative of the side chains in all non-glycine or proline amino acids), yet it is small enough to be studied thoroughly in the gas phase using high-level quantum chemical calculations[2] and in aqueous solution using classical computer simulations (Monte Carlo (MC) and molecular dynamics (MD)) or statistical mechanical integral equation theories.[3-8]

There have been several previous studies of the thermodynamics of conformational equilibria in the alanine dipeptide in water. Mezei et al.[4] used MC simulations to calculate the relative solvation thermodynamics of the C_{7ax}, α_R, and P_{II} ($\phi \approx -80°$, $\psi \approx 150°$) conformations. The full ϕ,ψ free energy surface for the dipeptide in water was determined in the studies by Pettitt and Karplus[6,7] and by Anderson and Hermans.[8] Pettitt and Karplus used a statistical mechanical integral equation theory, the extended RISM theory with a superposition approximation, to compute the free energy surface. Pettitt and Karplus also used finite difference temperature derivatives of the free energy to determine the corresponding internal energy and entropy surfaces. Anderson and Hermans employed MD simulations with specialized sampling methods to construct the conformational probability distribution from which they derived the free energy surface.

All three studies agree qualitatively in the sense that they all show that there is a marked solvent effect on conformational equilibria in the alanine dipeptide. Generally speaking, the aqueous solvent appears to "flatten" the ϕ,ψ free energy surface, decreasing the free energy difference between conformations that differed by large energies on the vacuum surface and lowering the barriers separating those conformations. It is interesting that the results of Anderson and Hermans for the dipeptide ϕ,ψ probability distribution in water actually match the observed protein distribution quite well.[8] This comparison suggests that the effects of the solvent on the conformational distribution of the dipeptide are similar to the effects of long-range and specific side chain interactions on the backbone in proteins. This profound global solvent modification of the conformational free energy surface affects not only the relative stabilities of the various conformations, but also the dynamics and fluctuations within the minima and the kinetics of interconversion of different species. Thus, we expect the solvent to play an important role in determining the mechanism of the folding/unfolding of small peptides in solution. Unfortunately, the quantitative details of the results of the three studies cited above differ, indicating a subtle model

† Present address: Department of Chemistry, University of Pennsylvania, Philadelphia, PA 19104.

(1) The alanine dipeptide is the blocked alanine residue, Ac-ala-NHMe, where Ac is the N-terminal blocking group, $COCH_3$, and NHMe is the C-terminal blocking group, $NHCH_3$.

(2) Head-Gordon, T.; Head-Gordon, M.; Frisch, M. J.; Brooks, C. L. III; Pople, J. A. *J. Am. Chem. Soc.* **1991**, *113*, 5989 and references therein.
(3) Rossky, P. J.; Karplus, M. *J. Am. Chem. Soc.* **1979**, *101*, 1913.
(4) Mezei, M.; Mehrotra, P. K.; Beveridge, D. L. *J. Am. Chem. Soc.* **1985**, *107*, 2239.
(5) Brady, J. Karplus, M. *J. Am. Chem. Soc.* **1985**, *107*, 6103.
(6) Pettitt, B. M.; Karplus, M. *Chem. Phys. Lett.* **1985**, *121*, 194.
(7) Pettitt, B. M.; Karplus, M. *J. Phys. Chem.* **1988**, *92*, 3994.
(8) Anderson, A.; Hermans, J. *Proteins* **1988**, *3*, 262.
(9) Tobias, D. J.; Brooks, C. L. III *Biochemistry* **1991**, *30*, 6059.

0022-3654/92/2096-3864$03.00/0

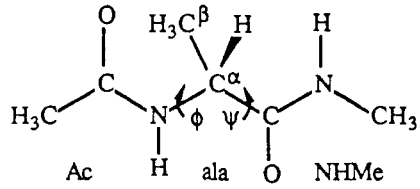

Figure 1. Chemical structure of the alanine dipeptide with the flexible backbone dihedral angles, ϕ and ψ, indicated. We label the N-terminal blocking group, Ac, as residue 1, the alanine residue as residue 2, and the C-terminal blocking group, NHMe, as residue 3.

and method dependence of the solvent effects.

Given the prominence of the dipeptide as a model for the protein backbone and the discrepancies between the previous studies of the dipeptide in water, we felt it was worthwhile to carry out a similar investigation using the models and methods we have employed in our studies of conformational equilibria in oligopeptides in solution.[9,10] By comparing the results of the present study and our previous work, we can see to what extent the backbone conformational equilibria in oligopeptides can be described in terms of independent pairs of ϕ and ψ dihedral angles.

In this paper, we study conformational equilibria in the alanine dipeptide to characterize the allowed and preferred conformations of the peptide backbone in the gas phase and in water. Of course, by using the dipeptide as a model for the peptide backbone, we are omitting long-range interactions (e.g., interactions reaching beyond nearest-neighbor residues in the sequence) of the backbone and specific side chain interactions. Clearly, these interactions are important in the conformational equilibria of oligopeptides and proteins in solution. Nonetheless, we can use the dipeptide to learn about the role of short-ranged backbone interactions (steric and hydrogen bonding) in determining the allowed and preferred backbone conformations and how the relative importance of these interactions is modified in aqueous solution.

We have used MD simulations with specialized sampling techniques to compute free energy profiles along paths connecting several conformations of the dipeptide on the ϕ,ψ surface in the gas phase and in water. By comparing the results from the vacuum and solution simulations, we have quantified the solvent effects on the conformational equilibrium. In addition, we have used thermodynamic decompositions of free energy differences into energetic and entropic contributions to understand the relative stabilities of the various conformations in terms of peptide–peptide and peptide–water interactions. We will also compare our results to the corresponding results determined previously using different models and methods. However, before we present our thermodynamic results, we will discuss the theoretical vacuum ϕ,ψ energy surfaces for several models of the dipeptide, and we briefly survey results from studies of the dipeptide in water.

Computational Methods

The potential energy function we employ, the CHARMM potential,[11] has an analytical form, with harmonic terms for bond stretching and bond angle and improper torsion bending, sinusoidal terms for dihedral angle rotation, and Lennard-Jones and Coulomb terms describing van der Waals and electrostatic interactions between atoms that are not bonded to each other (or are separated by at least three bonds). The CHARMM peptide parameters consist of force constants and equilibrium geometries derived from spectroscopic and crystallographic data and Lennard-Jones constants and atomic partial charges derived from ab initio quantum chemical calculations for small molecules.

To investigate the conformational equilibrium of the dipeptide in the gas phase, we constructed an adiabatic potential energy surface by using energies resulting from minimizing the CHARMM "polar hydrogen" potential with the addition of strong

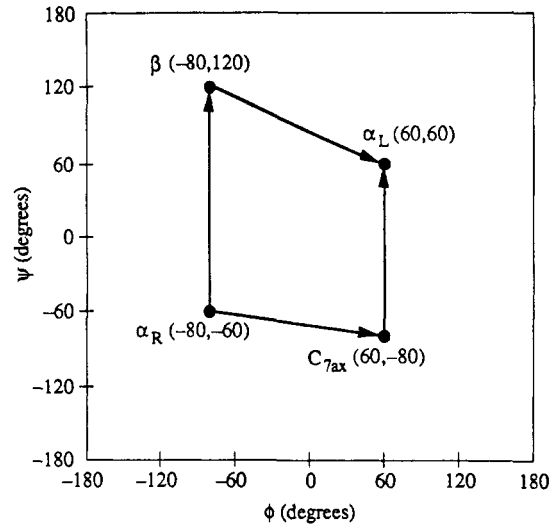

Figure 2. Definitions of the alanine dipeptide conformations (indicated by solid circles) and the paths (indicated by arrows) used in the free energy calculations.

harmonic constraint potentials on the ϕ and ψ dihedral angles. We used the PARAM19 parameters and default nonbonded energy truncation scheme (atom-based cutoffs at 7.5 Å with constant dielectric ($\epsilon = 1$), shifted Coulomb, and shifted Lennard-Jones terms[11]). Each minimization was carried out using the Powell algorithm[12] either for 500 steps or until the rms gradient was less than 0.005 kcal/(mol·Å^2) or the energy change was less than 0.001 kcal/mol. The minimizations were carried out at 10° intervals in ϕ and ψ.

For the purpose of the thermodynamic calculations in solution, it was convenient to define paths connecting the various conformers of interest. Our first step was to locate the conformers of the ϕ,ψ surface in solution. We decided to search for β sheet, α_R, α_L, and C_{7ax} conformations in water using the following procedure. We started with ideal structures and minimized their energy in the gas phase with strong harmonic constraints on ϕ and ψ. Then we placed each structure in a box of water and simulated it with periodic boundary conditions for 45 ps without constraints. The details of these simulations are given below. We used the peaks in the ϕ,ψ probability distributions (plotted on 10° square grids) from the four simulations to define the locations of the conformers in solution. The choices of the conformations and the paths used in the vacuum and solution thermodynamics calculations are shown in Figure 2.

For the calculation of the free energy profiles along the four paths, we used MD simulations with holonomic internal coordinate constraints[13] and thermodynamic perturbation theory (TPT).[14,15] In this approach, we perform a simulation with ϕ and ψ constrained at the values ϕ_i and ψ_i, respectively, and compute the Helmholtz free energy difference between systems with $(\phi,\psi) = (\phi_i,\psi_i)$ and $(\phi_i+d\phi,\psi_i+d\psi)$ using the following formula

$$\Delta A = A(\phi_i+d\phi_i,\psi_i+d\psi_i) - A(\phi_i,\psi_i)$$

$$= -\beta^{-1} \ln \langle \exp\{-\beta[U(\phi_i+d\phi_i,\psi_i+d\psi_i) - U(\phi_i,\psi_i)]\}\rangle_{\phi_i,\psi_i} \quad (1)$$

In eq 1, $\beta = 1/k_BT$, T is the absolute temperature, U is the potential energy (which depends on all of the peptide and solvent coordinates, although only the dependence on ϕ and ψ is indicated explicitly), and the $\langle ... \rangle_{\phi_i,\psi_i}$ denotes a statistical mechanical average over the canonical ensemble (constant number of atoms, volume, and temperature) where $(\phi,\psi) = (\phi_i,\psi_i)$. To compute the free energy profiles, we performed 15 simulations along the $\alpha_R \rightarrow \beta$ path with (ϕ,ψ) constrained at (-80°,-54°), (-80°,-42°), ..., (-80°,114°) and with $d\phi = 0$, $d\psi = \pm 3°, \pm 6°$; 10 simulations

(10) Tobias, D. J.; Sneddon, S. F.; Brooks, C. L. III *J. Mol. Biol.* **1991**, *216*, 783.
(11) Brooks, B. R.; Bruccoleri, R. E.; Olafson, B. D.; States, D. J.; Swaminathan, S.; Karplus, M. *J. Comput. Chem.* **1983**, *4*, 187.
(12) Powell, M. J. D. *Math. Programming* **1977**, *49*, 2574.
(13) Tobias, D. J.; Brooks, C. L. III *J. Chem. Phys.* **1988**, *89*, 5115.
(14) Zwanzig, R. *J. Chem. Phys.* **1954**, *22*, 1420.
(15) Tobias, D. J.; Brooks, C. L. III *Chem. Phys. Lett.* **1987**, *142*, 472.
(16) Jorgensen, W. L.; Chandrasekhar, J.; Madura, J.; Impey, R. W.; Klein, M. L. *J. Chem. Phys.* **1983**, *79*, 926.

along the $\alpha_R \rightarrow C_{7ax}$ path with $(\phi,\psi) = (-73°,-61°)$, $(-59°,-63°)$, ..., $(53°,-79°)$ and $d\phi = \pm 3.5°, \pm 7°$, $d\psi = \pm 0.5°, \pm 1°$; 10 simulations along the $C_{7ax} \rightarrow \alpha_L$ path with $(\phi,\psi) = (60°,-73°)$, $(60°,-59°)$, ..., $(60°,53°)$ and $d\phi = 0$, $d\psi = \pm 0.5°, \pm 1°$; and 10 simulations along the $\beta \rightarrow \alpha_L$ path with $(\phi,\psi) = (-73°,117°)$, $(-59°,111°)$, ..., $(53°,63°)$ and $d\phi = \pm 3.5°, \pm 7°$, $d\psi = \pm 1.5°, \pm 3°$. Thus, we obtained four free energy differences in each simulation, and we used 47 free energy values to construct the profile along the $\alpha_R \rightarrow \beta$ path and 32 values along the other three paths. We carried out four additional simulations, one at each corner of the circuit formed by the four paths, with holonomic ϕ and ψ constraints for the purpose of computing average interaction energies (see below).

To prepare a system for a solution simulation, we placed a single peptide molecule in the center of a box of water molecules and removed the water molecules that overlapped with the peptide atoms. Each system contained 202–207 water molecules. The box edge length, 18.856 Å, was chosen to yield approximate agreement with the experimentally observed room temperature water density (1.0 g·cm^{-3}) after the solute volume was subtracted from the box volume. All of the simulations were performed with periodic boundary conditions. We used the three-site TIP3P model of Jorgensen et al.[16] for water. The nonbonded energies and forces were smoothly truncated at 7.75 Å using a van der Waals switching function and an electrostatic shifting function,[11] based on atomic centers and according to the minimum image convention.[17] The Verlet algorithm[18] was used to integrate Newton's equations of motion (with a time step of 1.5 fs). Each vacuum or solution simulation (except for the four preliminary simulations described above) consisted of 5000 steps (7.5 ps) of equilibration and 10000 steps (15 ps) of data collection. The nonbonded interactions were processed using a list-based algorithm,[18] and the lists were updated every 10 steps. The velocities were periodically reassigned from a Maxwell–Boltzmann distribution to maintain temperatures of approximately 300 K. The SHAKE constraint algorithm[19] was used to keep the water molecules rigid and to maintain rigid N–H bonds in the peptide molecules, and the internal coordinate constraint algorithm[13] was used to keep peptide backbone dihedral angles fixed. The potential energies of each system were stored every time step for the calculation of the TPT free energy differences, and the coordinates were saved every five time steps for the calculation of the average interaction energies. All of the simulations were carried out using the CHARMM program[11] on the Cray YMP computer at the Pittsburgh Supercomputing Center.

In order to understand the relative free energies of the different conformations in solution in terms of microscopic interactions, it is useful to decompose free energy differences into energetic and entropic contributions arising from differences in peptide–peptide and peptide–water interactions.[10] The Helmholtz free energy difference between two conformational states may be written

$$\Delta A = \Delta E - T\Delta S \qquad (2)$$

where ΔE and ΔS are the differences in internal energy and entropy, respectively. The internal energy difference is equal to the difference of the average potential energies, which may be written as the sum of average peptide–peptide, peptide–water, and water–water interaction energy differences.[10] Similarly, the entropy difference may be decomposed into a configurational contribution arising from the peptide conformational fluctuations within the free energy wells[20] and peptide–water and water–water contributions which are comprised of complicated averages over peptide–water and water–water interactions, respectively.[21] The water–water energetic and entropic contributions exactly cancel for each conformation, and therefore they do not contribute to the free energy difference.[21] Thus, the thermodynamic decomposition may be written as follows

$$\Delta A = \langle \Delta U_{uu} \rangle + \langle \Delta U_{uv} \rangle - T\Delta S_{c,uv} \qquad (3)$$

where $\langle \Delta U_{uu} \rangle$ and $\langle \Delta U_{uv} \rangle$ are the average peptide–peptide and peptide–water interaction energy differences, respectively, and $\Delta S_{c,uv}$ is the sum of the peptide configurational and peptide–water entropy differences. For the potential energy function we use, the peptide–peptide interaction energy differences contain contributions from bond, angle, torsion, van der Waals, and electrostatic energies, while the peptide–water differences contain only van der Waals and electrostatic contributions. It is straightforward to compute the average interaction energies but difficult to calculate the entropy difference directly from the simulation data. Since the entropy contribution is the only missing term in eq 3, we obtain it indirectly as the difference between ΔA and the average interaction energies. Brady and Karplus[5] showed that the differences in configurational entropy between different conformations of the alanine dipeptide in ST2 water are small, ~0.5 kcal/mol of free energy at 300 K. Therefore, $\Delta S_{c,uv}$ is composed primarily of the difference in peptide–water entropy.

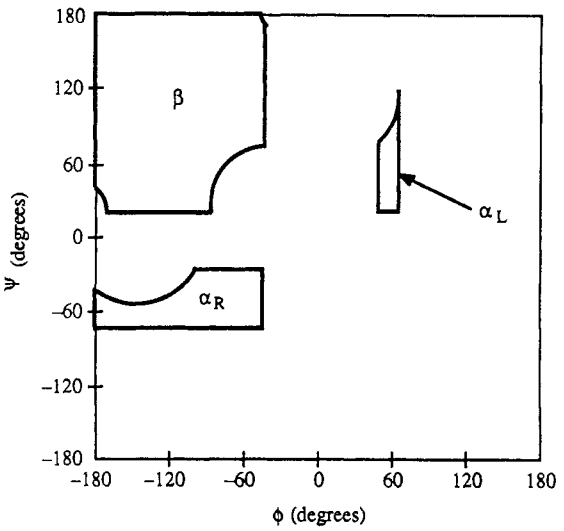

Figure 3. Simplified "derivation diagram" for the Ramachandran plot (after ref 23). The bold lines enclose the major allowed regions based on a hard-sphere model (ref 23). The pairs of atoms involved in the close contacts that lead to the forbidden regions are identified by Mandel et al.

Results and Discussion

The hard-sphere model is perhaps the simplest representation for the atoms in the dipeptide molecule. Consideration of the allowed (e.g., zero potential energy) and forbidden (e.g., infinite potential energy) regions of the Ramachandran map[22] based on a hard-sphere model for the dipeptide leads to the so-called "derivation diagram".[23] In Figure 3 we show a schematic version of the derivation diagram.

The clashes between several different pairs of hard-sphere atoms produce large forbidden regions.[23] For example, the region near the center of the plot is forbidden because the oxygen atom of residue 1 collides with the carbonyl carbon atom of residue 2. Three significant allowed regions remain: a large region (labeled β) in the $(-\phi,+\psi)$ quadrant containing the ideal β sheet and polyproline conformations, a smaller region (labeled α_R) in the $(-\phi,-\psi)$ quadrant containing the ideal right-handed α helical conformations, and an even smaller region (labeled α_L) in the $(+\phi,+\psi)$ quadrant containing the ideal left-handed α helical

(17) Allen, M. P.; Tildesley, D. J. *Computer Simulation of Liquids*, pbk ed.; Oxford University Press: Oxford, 1989.
(18) Verlet, L. *Phys. Rev.* **1967**, *159*, 98.
(19) Ryckaert, J.-P.; Ciccotti, G.; Berendsen, H. J. C. *J. Comput. Phys.* **1977**, *23*, 327.
(20) Karplus, M.; Ichiye, T.; Pettitt, B. M. *Biophys. J.* **1987**, *52*, 1083.
(21) Yu, H.-A.; Karplus, M. *J. Chem. Phys.* **1988**, *89*, 2366.
(22) Ramachandran, G. N.; Sasisekharan, V. *Adv. Protein Chem.* **1968**, *23*, 284.
(23) Mandel, N.; Mandel, G.; Trus, B. L.; Rosenberg, J.; Carlson, G.; Dickerson, R. E. *J. Biol. Chem.* **1977**, *252*, 4619.
(24) Richardson, J. S. *Adv. Protein Chem.* **1981**, *34*, 167.

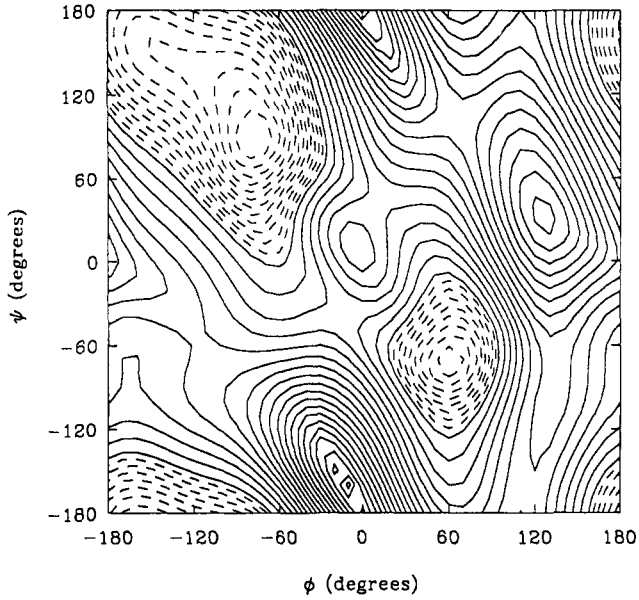

Figure 4. CHARMM potential energy as a function of the ϕ and ψ dihedral angles in the alanine dipeptide. Dashed contours are drawn at 0.5 kcal/mol intervals to 7.0 kcal/mol. Solid contours are drawn at 1.0 kcal/mol intervals.

conformations. Richardson[24] has noted that the outlines of the allowed regions "fit the distribution [of ϕ,ψ pairs for non-glycine residues] in proteins fairly well, except for the rather frequent occurrence of residues in the bridge region between the α_R and β regions". The bridge region becomes allowed if the C–C_α–N bond angle increases from its ideal value.[22]

A more refined ϕ,ψ energy surface can be calculated using a suitably parametrized empirical potential energy function. We show an adiabatic ϕ,ψ energy surface for the alanine dipeptide in Figure 4. The empirical energy surface for the dipeptide in the gas phase differs from the derivation diagram and the observed distribution of ϕ,ψ angles in proteins (for example, see the distribution of ϕ,ψ angles for approximately 1000 non-glycine residues from high-resolution crystal structures of eight proteins plotted by Richardson[24]) in a few important respects. First of all, there are no relative minima on the empirical surface corresponding to the right- or left-handed α helices. In addition, the right-handed α helical conformations are much higher in energy compared to β conformations than we would predict by looking at the relative populations of ϕ,ψ pairs in the α and β regions in a Ramachandran plot for globular proteins. Furthermore, there is a relative minimum centered at $\phi,\psi \approx 60°$–$80°$ on the empirical energy surface, corresponding to the so-called C_{7ax} conformation. This conformation is not allowed on the derivation diagram, and the region around it is not populated in the protein distribution. The only obvious similarity between the energy surface, the derivation diagram, and the protein distribution is the broad region of stable β conformations. However, the β well on the empirical energy surface is deeper and steeper than the relatively flat surface we expect based on the flat distribution of β conformations in proteins. These differences should not be too surprising since we are comparing a gas-phase potential to a protein potential of mean force.

A more rigorous theoretical description of the conformational energetics of the dipeptide may be obtained by using quantum chemical calculations which allow the electron distribution of the molecule to change with the conformation. Several quantum chemical studies of the alanine dipeptide energy surface have been carried out.[2] We only consider the calculations of Head-Gordon et al.[2] here since they are the most sophisticated to date. (For a comparison of these calculations to previous work, see ref 25.)

TABLE I: Comparison of the Geometries and Energies of the Three Lowest Energy Minima on Empirical and ab Initio Quantum Chemical ϕ,ψ Energy Surfaces for the Alanine Dipeptide in the Gas Phase[a]

conformation[b]	empirical[c] ϕ	empirical[c] ψ	empirical[c] energy	quantum chemical[d] ϕ	quantum chemical[d] ψ	quantum chemical[d] energy
C_{7eq}	−77.5	89.9	0	−85.8	78.1	0
C_5	−134.8	145.9	1.78	−204.4	199.8	1.13
C_{7ax}	60.6	−72.4	2.00	75.1	−54.2	2.19

[a] Dihedral angles are given in degrees and energies in kcal/mol. [b] For drawings of the peptide in these conformations, see ref 25. [c] CHARMM potential energy function with the PARAM19 "polar hydrogen" parameters and default nonbonded energy truncation scheme (described in the text). [d] Ab initio MP2/6-31+G** energies computed at HF/6-31+G* optimized geometries (ref 25) for a dipeptide analogue in which the methyl groups in the blocking groups of the alanine dipeptide have been replaced by hydrogen atoms.

Head-Gordon et al. studied several conformations of the alanine dipeptide and an "alanine dipeptide analogue", in which the Ac and NHMe methyl groups were replaced by hydrogen atoms, using ab initio quantum chemical methods[26] at the Hartree–Fock (HF) level with two different model basis sets, STO-3G and 3-21G, and concluded that the conformational energetics of the dipeptide and the analogue were virtually indistinguishable. They examined the integrity of 3-21G basis by characterizing several minima on the ϕ,ψ surface of the dipeptide analogue at larger basis sets, with and without electron correlation (included by using second-order Møller–Plesset perturbation theory (MP2)). They found that with the larger basis sets the minimum-energy geometries changed a little, but the energetics were unaffected qualitatively, even when electron correlation was included. They proceeded to generate the full ϕ,ψ energy surface using 3-21G energies minimized with respect to all other geometric variables at 30° intervals in ϕ and ψ.

The surface plotted in Figure 4 of the paper by Head-Gordon et al.[2] bears a striking resemblance to the empirical CHARMM surface we plotted in Figure 4. Not only are the overall topographies (e.g., the number of extrema and their locations) of the two surfaces very similar, but so are the ordering and relative energies of the three lowest minima on each surface (Table I). The most noticeable difference is the ϕ,ψ values for the C_5 conformation (Table I). However, as Head-Gordon et al. noted, the surface is very flat in the region of the C_5 conformation, so that differences in the precise location of the C_5 conformation are not very significant. Finally, we note that even the heights of the barriers separating the minima on the two surfaces are quite similar. For example, the barrier for the transition between the C_{7eq} and C_{7ax} conformations is approximately 10 kcal/mol on both surfaces. We conclude from this comparison of the CHARMM and 3-21G ab initio energy surfaces that the CHARMM potential provides a very good description of peptide–peptide interactions involving the peptide backbone.

On the basis of a comparison of the empirical and quantum chemical energy surfaces with the observed distribution of ϕ,ψ angles in proteins, we conclude that the dipeptide in the gas phase is not a very good model for the peptide backbone in proteins. Furthermore, we deduce that the long-range backbone and specific side chain interactions, as well as possible interactions with the solvent, are definitely important in determining the backbone conformations of proteins. Next, we briefly survey previous studies concerned with the effects of aqueous solvent on the conformational thermodynamics of the alanine dipeptide.

In Figure 5 we show the free energy profiles along the four paths in the gas phase and in solution. The statistical errors in the free energy differences used to construct the profiles, derived by error propagation from the standard deviations of the averages in eq 1 (determined using the method of batch averages[27] with a batch size of 100 data sets), are quite small (a few hundredths of

(25) Head-Gordon, T.; Head-Gordon, M.; Frisch, M. J.; Brooks, C. III; Pople, J. *Int. J. Quantum Chem., Quantum Biol. Symp.* **1989**, *16*, 311.
(26) Hehre, W. J.; Radom, L.; Schleyer, P. R.; Pople, J. A. *Ab Initio Molecular Orbital Theory*, Wiley-Interscience: New York, 1986.
(27) Wood, W. W. In *Physics of Simple Liquids*; Rowlinson, J. S., Rushbrooke, G. S., Eds.; North-Holland: Amsterdam, 1968.
(28) Deleted in proof.

TABLE II: Relative Free Energies of Various Alanine Dipeptide Conformations in the Gas Phase and in Water[a]

conformation	ϕ	ψ	ΔA_{vac}	ΔA_{wat}
β	−80	120	0	0
α_R	−80	−60	9.1	0.2
α_L	60	60	11.6	4.1
C_{7ax}	60	−80	2.4	3.6

[a] Free energy values given relative to the β conformation in kcal/mol; angles in degrees.

TABLE III: Thermodynamic Decompositions of the Relative Free Energies of Various Alanine Dipeptide Conformations in Water[a]

conformation	ΔA	ΔE_{uu}	ΔE_{uv}	$-T\Delta S_{c,uv}$
β	0	0	0	0
α_R	0.2	11.8	−15.9	4.3
α_L	4.1	13.8	−18.4	8.7
C_{7ax}	3.6	2.7	0.8	0.1

[a] Values given relative to the β conformation in kcal/mol.

kcal/mol). A better measure for the errors in the profiles is the so-called "closure error",[29] the sum of the free energy differences between the end points for the four paths, which should add up to zero since the free energy is a state function and the four paths complete a closed thermodynamic cycle. The closure error is 0.46 kcal/mol in the vacuum data and 0.58 kcal/mol in the solution data. We consider these closure errors to be upper bounds on the errors in any free energy differences taken from the free energy profiles.

The relative free energies of the four conformations, taken from the profiles, are summarized in Table II. These results should be regarded as approximate, since we did not determine the full ϕ,ψ free energy surfaces and therefore do not know exactly where the minima (if they exist) are. Also, by constraining both ϕ and ψ in the simulations, we are missing some of the entropic contribution that might arise from motion orthogonal to the paths.[30] Nonetheless, we are confident that the results give a qualitatively correct picture of the solvent effects on the conformational equilibrium.

We can make several statements regarding the dipeptide conformational equilibrium based on the data in Table II and Figure 5. Both in the gas phase and in water, the β conformation is the most stable and the α_L conformation is the least stable (Table II). Overall, the differences in stability are attenuated by solvation: the free energy difference between the most and least stable conformations is 11.6 kcal/mol in the gas phase but only 4.1 kcal/mol in water. Both the right- and left-handed α helical conformations are much less unstable relative to the β conformation in solution. In contrast, the C_{7ax} conformation is destabilized relative to the β conformation in solution, most likely because the hydrogen bond (closing the seven-membered ring) that strongly stabilizes the C_{7ax} in the gas phase is weakened by solvation. Finally, looking at the free energy profiles (Figure 5), we se that the underlying free energy surface appears much flatter in solution compared to in the gas phase.

In Table III we show the thermodynamic decompositions of the relative free energies in water. The statistical uncertainties (taken as the standard deviations of the averages determined using the method of batch averages with a batch size of 100 data sets) range from 1.8 to 3.0 kcal/mol in the peptide–peptide energy differences and 4.8–8.0 kcal/mol for the peptide–water energy differences. The uncertainties in the entropic contributions, determined by error propagation, range from 5.2 to 8.5 kcal/mol.

The data in Table III show that the α helical and C_{7ax} conformations are destabilized energetically relative to the β conformation by peptide–peptide interactions, although the desta-

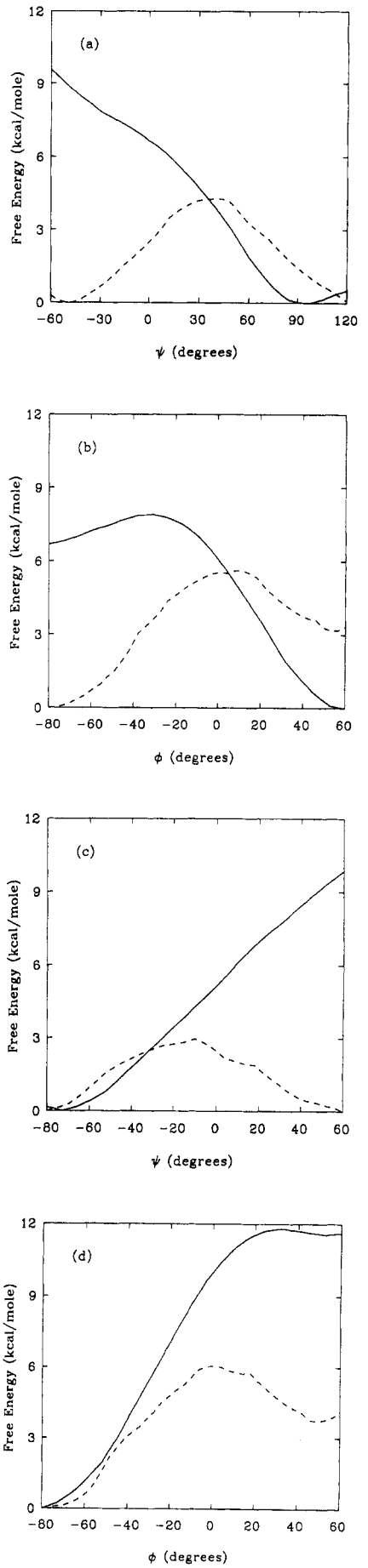

Figure 5. Free energy profiles along paths in the gas phase (solid curve) and in water (broken curve) connecting (a) α_R and β, (b) α_R and C_{7ax}, (c) C_{7ax} and α_L, and (d) β and α_L.

(29) Hermans, J.; Yun, R.-H.; Anderson, A. G. In *Crystallographic and Modelling Methods in Molecular Design*; Bugg, C. E., Ealick, S. E., Eds.; Springer-Verlag: New York, 1990.

(30) Lazaridis, T.; Tobias, D. J.; Brooks, C. L. III; Paulaitis, M. *J. Chem. Phys.* **1991**, *95*, 7612.

TABLE IV: Comparison of Theoretical Results for the Relative Free Energies of Various Alanine Dipeptide Conformations in Water[a]

	ΔA		
conformation	Anderson and Hermans (MD)	Pettitt and Karplus (RISM)	this work
α_R	0	0	0
β	−1.4		−0.2
α_L	1.1	−0.7	3.8
C_{7ax}	1.4	−1.8	3.3

[a] Values given relative to the α_R conformation in kcal/mol.

bilization is much greater for the helical conformations. This destabilization is more than compensated in the helical conformations, but only slightly compensated in the C_{7ax} conformation, by the peptide–water interaction energy. The entropic contribution favors the β conformation significantly over the helical conformations but not over the C_{7ax} conformation.

By looking at the contributions to the interaction energy differences from the various energy terms, we have arrived at a microscopic interpretation for the thermodynamic decompositions. Most of the peptide–water interaction energy difference (~9 kcal/mol) for both the helical conformations comes from the electrostatic contributions. This is because the peptide unit dipoles are essentially antiparallel in the β conformation, but they are aligned in the helical conformations. Thus, the change from β to helical conformations is accompanied by a large, positive change in the peptide electrostatic energy. The additional destabilization (~3 kcal/mol) due to peptide–peptide interactions in the α_L conformation arises from unfavorable van der Waals interactions and angle strain due to close contacts between the β carbon and the acetyl carbonyl oxygen atom. The peptide unit dipoles are also approximately aligned in the C_{7ax} conformation. However, in contrast to the helical conformations, the dipoles in the C_{7ax} conformation are in a "head-to-tail" hydrogen-bonding arrangement. The electrostatic contribution to the peptide–peptide energy difference actually favors C_{7ax} over β by about a kcal/mol. The overall slight destabilization is due to van der Waals and angle strain, which amount to ~3 kcal/mol in the C_{7ax} conformation. The dipole moment of the whole molecule is greater in the helical and C_{7ax} conformations than in the β conformation because the peptide dipoles are aligned in the helical and C_{7ax} conformations. Thus, the helical conformations "bind" more waters than the β, reducing the peptide–water entropy, leading to a significant, positive entropic contribution to the free energy differences. Evidently, this does not occur in the C_{7ax} conformation because of the intramolecular hydrogen bond.

It would be nice if we could compare our results to those from experimental studies. Several studies of the dipeptide in solution have been reported.[31-33] These studies indicate that the conformational equilibrium cannot be described by a simple one- or two-state model, but unfortunately, they do not provide results for the relative populations of the various conformations in solution.

We can compare our results to the results of previous theoretical studies of the dipeptide in solution. In Table IV we compare the relative free energies of various conformations in water from our work to the MD results of Anderson and Hermans[8] and the integral equation results of Pettitt and Karplus.[7] We only tabulated the results from other studies for conformations that corresponded closely to the ones we studied. We did not include the MC results of Mezei et al.[4] in Table IV because they do not include the peptide–peptide contributions.

All of the results in Table IV agree qualitatively in the sense that there is a substantial solvent effect on the backbone conformational equilibrium. The ordering of the stabilities is the same, and the magnitudes are similar, in our work and the work of Anderson and Hermans. However, Pettitt and Karplus found the opposite ordering of the stabilities of the helical and C_{7ax} conformations. The agreement of our results with the results of Anderson and Hermans is quite good, especially considering that we used different models and methods.

TABLE V: Comparison of Theoretical Results for the Relative Solvation Free Energies of Various Alanine Dipeptide Conformations in Water[a]

	ΔA_{solv}		
conformation	Mezei et al. (MC)	Pettitt and Karplus (RISM)	this work
α_R	0	0	0
β	0.4		8.8
α_L		−0.5	1.3
C_{7ax}		9.2	10

[a] Values given relative to the α_R conformation in kcal/mol.

In Table V we compare the relative solvation free energies, $\Delta A_{solv} = \Delta A_{water} - \Delta A_{vacuum}$, for our work with the MC results of Mezei et al. and the integral equation results of Pettitt and Karplus. We did not include results from Anderson and Hermans because they did not provide the vacuum energy differences for their model.

Given the uncertainties, our results for the solvation free energies agree quite well with the results of Pettitt and Karplus: both studies predict that two α helical conformations have similar solvation free energies, although we predict that α_R is slightly more favorably solvated than α_L, while Pettitt and Karplus predict the opposite; and both predict that the helical conformations are much more favorably solvated than the C_{7ax} conformation. Mezei et al. predict that the solvation of the β conformation is more favorable than the α_R conformation, but to a much lesser extent than we predict.

Finally, we compare the peptide–water internal energies of solvation, ΔE_{uv}, from our work and the study of Mezei et al. for the $\beta \rightarrow \alpha_R$ transition. We obtained −15.9 kcal/mol (Table III) while Mezei et al. obtained 1.1 kcal/mol. Thus, as in the case of the solvation free energies, we find that the agreement between our results and those of Mezei et al. is not very good. There are several possible reasons for such a large discrepancy: slightly different definitions of the conformations, large uncertainties in average interaction energies, different models and sampling techniques. It is difficult to say what is the major reason for the differences between our results and the results of Mezei et al. The discrepancies underscore the sensitivity of the results of the details of the models and methods employed in thermodynamics calculations via computer simulations.

Conclusions

As we expected after seeing the results of previous work, our results show that there are marked solvent effects on the backbone conformational equilibrium in the alanine dipeptide. We anticipate that the same effects will operate on longer peptides. Furthermore, hydrophobic effects, which we have not considered here because they do not really influence the conformational equilibrium in the dipeptide, are thought to be the dominant stabilizing force in folded proteins.[34] Clearly, solvent effects are important in proteins. Since many proteins attain their biologically active conformation and function in aqueous solution, most biologically relevant theoretical studies of these proteins (e.g., studies of processes occurring on the surfaces of proteins or in exposed active sites, folding events, etc.) must therefore include realistic solvent effects. An exception would be the case of studies of the interior of a folded protein, assuming the structure is properly maintained in the absence of solvent.[35] Ab initio calculations on small peptides are useful for the purposes of developing potential functions, but since it is presently not possible to incorporate realistic solvent effects into the calculations, in themselves these calculations are not very useful for understanding the stability of folded proteins or the confor-

(31) Avignon, A.; von Huang, P. *Biopolymers* **1970**, *9*, 427.
(32) Avignon, A.; Garrigou-Lagrange, C.; Botherel, D. *Biopolymers* **1973**, *12*, 1651.
(33) Madison, V.; Kopple, K. D. *J. Am. Chem. Soc.* **1980**, *102*, 4855.
(34) Dill, K. A. *Biochemistry* **1990**, *29*, 7133.
(35) Berendsen, H. J. C. In *Molecular Dynamics and Protein Structure*; Hermans, J., Ed.; Polycrystal Book Service: Western Springs, 1985.

mational equilibria in peptides in solution. Likewise, vacuum molecular mechanics, Monte Carlo (MC), or molecular dynamics (MD) calculations with empirical potential energy functions have limited utility in the study of biologically relevant problems. The current best theoretical approach is to carry out MC or MD simulations based on an accurate, empirical potential energy function containing terms that describe interactions between the protein atoms and the atoms explicitly modeled solvent molecules.

Acknowledgment. This work was partially supported by an NIH Grant to C.L.B. (GM37554). C.L.B. was an A. P. Sloan Foundation Fellow (1990-1992). D.J.T. was supported by an NIH predoctoral training grant. We are grateful to the NSF for a generous grant of computer time at the Pittsburgh Supercomputing Center.

Registry No. Ac-Ala-NHMe, 19701-83-8.

Resonance Raman Characterization of Polarons and Bipolarons in Sodium-Doped Poly(*p*-phenylenevinylene)

Akira Sakamoto, Yukio Furukawa, and Mitsuo Tasumi*

Department of Chemistry, Faculty of Science, The University of Tokyo, Bunkyo-ku, Tokyo 113, Japan
(Received: November 18, 1991)

The resonance Raman spectra of sodium-doped poly(*p*-phenylenevinylene) (PPV) and the radical anions and dianions of three model compounds $CH_3(C_6H_4CH{=}CH)_nC_6H_4CH_3$ (PV*n*, n = 1-3) have been studied. The Raman spectra of sodium-doped PPV show marked changes with laser wavelengths used for Raman excitation. These spectra have been analyzed on the basis of the resonance Raman spectra of the radical anions and dianions of the model compounds, which correspond, respectively, to negative polarons and bipolarons in PPV. Three kinds of negative polarons whose lengths are close to PV1, PV2, and PV3, and a bipolaron which is localized in a region close to PV3, exist in a sodium-doped PPV film. Upon prolonged heat treatment of the sodium-doped PPV (290 °C, 12 h), the shortest polaron corresponding to the radical anion of PV1 disappears, probably because it combines with another polaron to form a bipolaron. These results indicate that resonance Raman spectroscopy is a powerful tool for characterizing polarons and bipolarons in conducting polymers.

Introduction

Poly(*p*-phenylenevinylene) (Figure 1a, abbreviated as PPV) has attracted the attention of researchers interested in conjugated polymers because of its nonlinear optical properties[1] and high electrical conductivities upon doping.[2-6] The electrical conductivity of a highly stretched film of PPV has been reported to become as high as 1.12×10^4 S cm^{-1} when treated with concentrated sulfuric acid (p-type doping)[5] and 2.0×10^3 S cm^{-1} when doped with sodium (n-type doping).[6]

The mechanism of electrical conduction in conducting polymers has been discussed in terms of the self-localized excitations (such as solitons, polarons, and bipolarons) created upon doping.[7] Since the ground state of PPV is nondegenerate, the polarons and bipolarons are considered to be the intrinsic excitations in this polymer. When an electron is added to a conjugated polymer chain, a radical anion extending over a certain number of repeating units is created. Some examples of such radical anions, which are called negative polarons, are schematically depicted in Figure 2a-c. If another electron is added to the already reduced polymer chain containing the negative polarons, either another independent polaron or a dianion without an unpaired electron would be created. The dianions to be produced from the negative polarons in Figure 2a-c are depicted in Figure 2d-f. These dianions are called negative bipolarons.

The main problem in the structural study of doped conducting polymers is to elucidate the types and regions (lengths) of the self-localized excitations (polarons and bipolarons in the case of PPV) created upon doping. Since polarons and/or bipolarons are considered to be the charge carriers in conducting polymers with nondegenerate ground states, it is important to characterize these self-localized excitations for understanding the mechanism of electrical conduction.

In our recent studies[8,9] on the spectral characteristics of PPV and its model compounds $CH_3(C_6H_4CH{=}CH)_nC_6H_4CH_3$ (PV*n*, n = 1-3, shown in Figure 1b-d), we have demonstrated that these model compounds are very useful for understanding the vibrational spectra and structure of PPV in the pristine state. It is then conceivable that the radical ions and divalent ions derived from the model compounds may also give crucial information for clarifying the spectral characteristics of the polarons and bipolarons in the doped PPV.[10-14] The radical anions of PV*n*'s correspond to the negative polarons (NP*n*) in Figure 2a-c, and the dianions of PV*n*'s to the negative bipolarons (NBP*n*) in Figure 2d-f.

It has been reported that the electronic absorption of sodium-doped PPV appears in the region from visible to near-infrared.[15]

(1) Kaino, T.; Kubodera, K.; Tomaru, S.; Kurihara, T.; Saito, S.; Tsutsui, T.; Tokito, S. *Electron. Lett.* **1987**, *23*, 1095.
(2) Murase, I.; Ohnishi, T.; Noguchi, T.; Hirooka, M. *Polym. Commun.* **1984**, *25*, 327.
(3) Gagnon, D. R.; Capistran, J. D.; Karasz, F. E.; Lenz, R. W. *Polym. Bull.* **1984**, *12*, 293.
(4) Murase, I.; Ohnishi, T.; Noguchi, T.; Hirooka, M. *Synth. Met.* **1987**, *17*, 639.
(5) Hirooka, M.; Murase, I.; Ohnishi, T.; Noguchi, T. In *Frontiers of Macromolecular Science*; Saegusa, T., Ed.; Blackwell Scientific Publications: Oxford, U.K., 1989; p 425.
(6) Chen, D.; Winokur, M. J.; Masse, M. A.; Karasz, F. E. *Phys. Rev. B* **1990**, *41*, 6759.
(7) Heeger, A. J.; Kivelson, S.; Schrieffer, J. R.; Su, W.-P. *Rev. Mod. Phys.* **1988**, *60*, 781.
(8) Furukawa, Y.; Sakamoto, A.; Tasumi, M. *J. Phys. Chem.* **1989**, *93*, 5354.
(9) Sakamoto, A.; Furukawa, Y.; Tasumi, M. *J. Phys. Chem.* **1992**, *96*, 1490.
(10) Spangler, C. W.; Hall, T. J.; Sapochak, L. S.; Liu, P.-K. *Polymer* **1989**, *30*, 1166.
(11) Schenk, R.; Gregorius, H.; Meerholz, K.; Heinze, J.; Müllen, K. *J. Am. Chem. Soc.* **1991**, *113*, 2634.
(12) Oberski, J. M.; Greiner, A.; Bässler, H. *Chem. Phys. Lett.* **1991**, *184*, 391.
(13) Furukawa, Y. In *Electronic Properties of Conjugated Polymers*; Springer Ser. Solid-State Sci.; Kuzmany, H., Mehring, M., Roth, S., Eds.; Springer-Verlag: Berlin, in press.
(14) Furukawa, Y.; Sakamoto, A.; Ohta, H.; Tasumi, M. *Synth. Met.*, in press.

0022-3654/92/2096-3870$03.00/0